

**Supporting information for:**

**Direct Detection of Point Mutations in Non-amplified Human Genomic DNA**

Roberta D'Agata,<sup>†</sup> Giulia Breveglieri,<sup>§</sup> Laura M. Zanolì,<sup>||</sup> Monica Borgatti,<sup>§</sup> Giuseppe Spoto,<sup>\*,†,‡</sup> and Roberto Gambari<sup>\*,§,#</sup>

<sup>†</sup> Dipartimento di Scienze Chimiche, Università di Catania, Viale Andrea Doria 6, I-95125 Catania, Italy

<sup>§</sup> Centro di Biotecnologie, Università di Ferrara, via Fossato di Mortara 64b, 44121 Ferrara, Italy

<sup>||</sup> Scuola Superiore di Catania, c/o Dipartimento di Scienze Chimiche, Università di Catania, Viale Andrea Doria 6, Catania, Italy

<sup>‡</sup> Istituto Biostrutture e Bioimmagini, CNR, Viale A. Doria 6, Catania, Italy

<sup>#</sup> Dipartimento di Biochimica e Biologia Molecolare, via Fossato di Mortara 74, 44121 Ferrara, Italy

Table S1. Genomic DNA samples.		
	Thalassemia mutation	Stock solution concentration (ng $\mu\text{L}^{-1}$ )
Sample 1	$\beta\text{N}/\beta\text{N}$	128.4
Sample 2	$\beta^{\circ}39 \text{ C}>\text{T}$ heterozygous, $\beta^{\circ}39/\beta\text{N}$	629.0
Sample 3P	$\beta\text{N}/\beta\text{N}$	72.5
Sample 4	$\beta^{\circ}39 \text{ C}>\text{T}$ homozygous, $\beta^{\circ}39/\beta^{\circ}39$	17.0
Sample 5	$\beta^{\circ}39 \text{ C}>\text{T}$ heterozygous, $\beta^{\circ}39/\beta\text{N}$	133.0
Sample 6	$\beta^{\circ}39 \text{ C}>\text{T}$ homozygous, $\beta^{\circ}39/\beta^{\circ}39$	101.3
Sample 7	$\beta^{\circ}39 \text{ C}>\text{T}$ heterozygous, $\beta^{\circ}39/\beta\text{N}$	94.3
Sample 8	$\beta^{\circ}39 \text{ C}>\text{T}$ homozygous, $\beta^{\circ}39/\beta^{\circ}39$	120.0
Sample 9	$\beta^{\circ}39 \text{ C}>\text{T}$ homozygous, $\beta^{\circ}39/\beta^{\circ}39$	218.4
Sample 12	$\beta^{\circ}39 \text{ C}>\text{T}$ heterozygous, $\beta^{\circ}39/\beta\text{N}$	196.8
Sample 13	$\beta^{\circ}39 \text{ C}>\text{T}$ homozygous, $\beta^{\circ}39/\beta^{\circ}39$	132.0
Sample 14	$\beta^{\circ}39 \text{ C}>\text{T}$ heterozygous, $\beta^{\circ}39/\beta\text{N}$	230.4
Sample 18	$\beta^{\circ}39 \text{ C}>\text{T}$ homozygous, $\beta^{\circ}39/\beta^{\circ}39$	84.0
Sample 20	$\beta^{\circ}39 \text{ C}>\text{T}$ heterozygous, $\beta^{\circ}39/\beta\text{N}$	177.6
Sample 21	$\beta^{\circ}39 \text{ C}>\text{T}$ homozygous, $\beta^{\circ}39/\beta^{\circ}39$	42.0
Sample 26	$\beta^{\circ}39 \text{ C}>\text{T}$ heterozygous, $\beta^{\circ}39/\beta\text{N}$	101.0
Sample 82	$\beta\text{N}/\beta\text{N}$	102.0
Sample 83	$\beta\text{N}/\beta\text{N}$	293.5

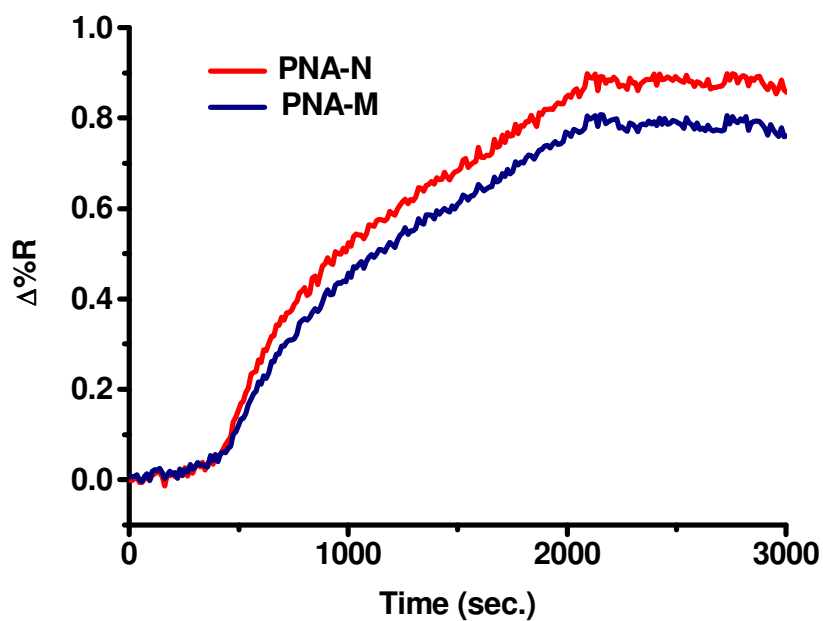


**Figure S1.** Representative changes in percent reflectivity ( $\Delta\%R$ ) over time obtained for the immobilization of PNA-N and PNA-M probes ( $0.1 \mu\text{M}$  in PBS).

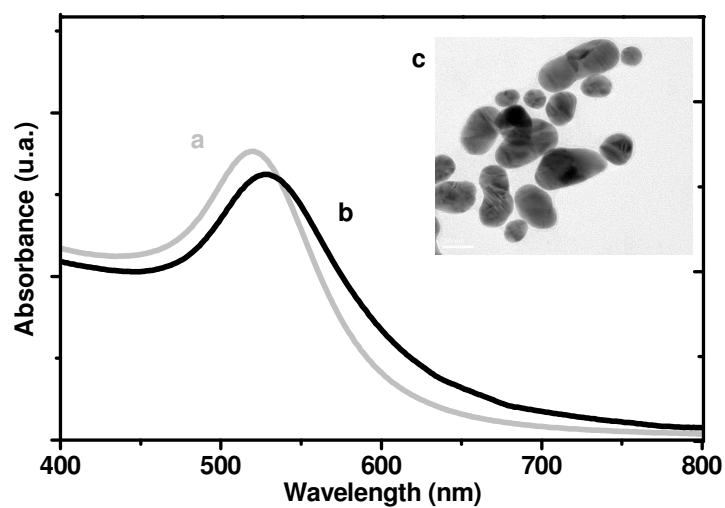


**Figure S2.** Representative UV-vis spectra of the citrate-stabilized AuNPs before ( $\lambda_{\text{max}} = 520 \pm 1 \text{ nm}$ ) (a) and after ( $\lambda_{\text{max}} = 528 \pm 1 \text{ nm}$ ) (b) the functionalization with DNA $\beta$ 39 11-mer oligonucleotide. (c) TEM image of AuNPs (mean diameter =  $20 \pm 5 \text{ nm}$ ).

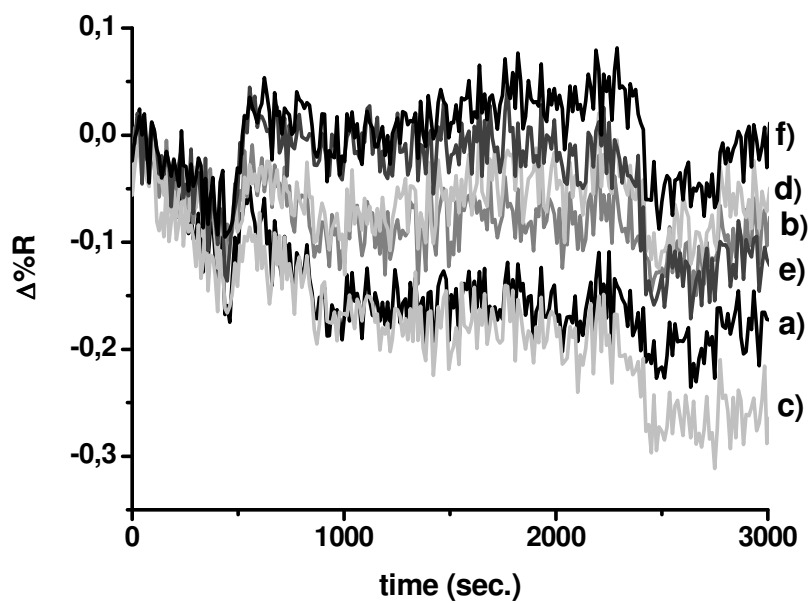


**Figure S3.** Representative change in percent reflectivity ( $\Delta\%R$ ) over time obtained for the interaction between surface immobilized PNA-N (**a,c, e**) and PNA-M (**b, d, f**) probes and  $5 \text{ pg } \mu\text{L}^{-1}$  DNA samples (**a, b** homozygous), (**c, d** wild-type), (**e, f** heterozygous).

Nanoparticle enhancement of SPRI signal and PCR-free detection of human point mutations using genomic DNA

**Fig. S4-S9** show some representative SPRI responses obtained when conjugated AuNPs were adsorbed on normal, heterozygous and homozygous DNA samples previously adsorbed on PNA-N and PNA-M surfaces. **Fig. S3** shows a further set of measurements. SPR difference images for each experiment are also shown. **Fig. S9** shows only four channels instead of six because the formation of air bubbles in one of the two missing microchannels altered the integrity of the chip surface.

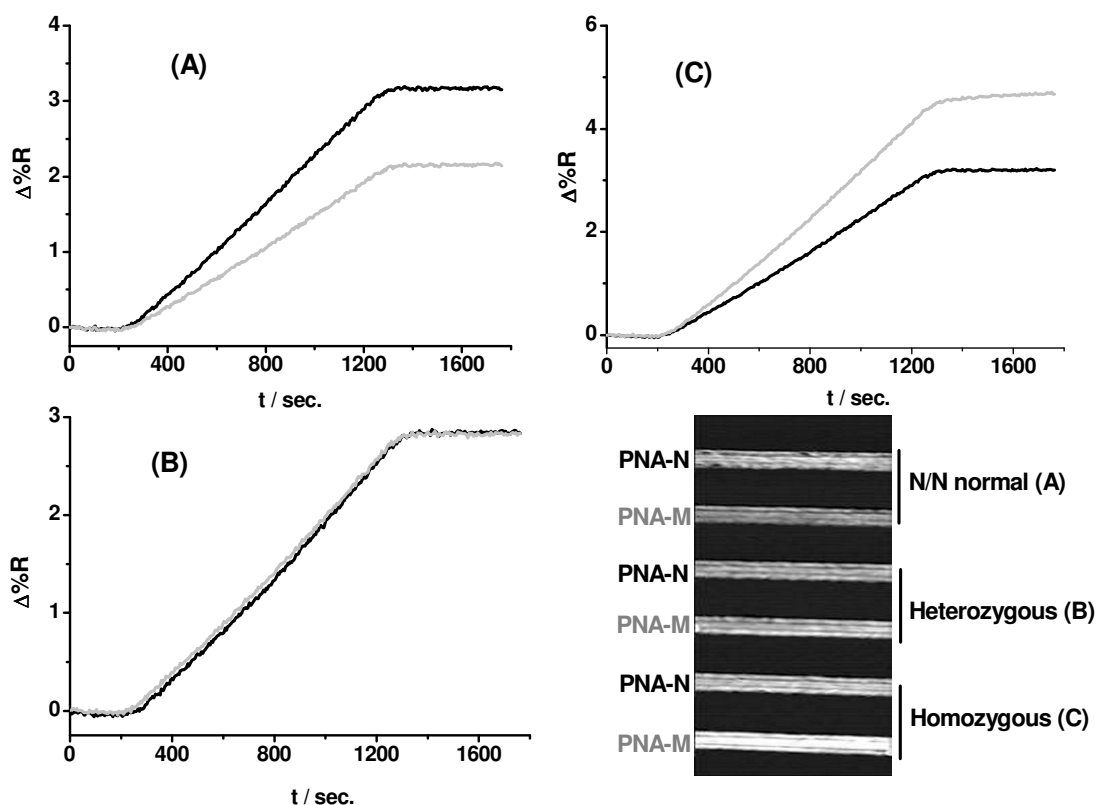


**Figure S4** Time-dependent SPRI curves obtained after the adsorption of conjugated AuNPs on normal  $\beta^N/\beta^N$  (A, sample 82), heterozygous  $\beta^{39}/\beta^N$  (B, sample 2) and homozygous  $\beta^{39}/\beta^{39}$  (C, sample 4) DNAs previously adsorbed to the surface immobilized PNA-N (black curve) and PNA-M (gray curve) probes.  $5 \text{ pg } \mu\text{L}^{-1}$  solutions of genomic DNAs were used for the experiments. A representative SPR difference image is also shown. In order to prevent memory effects the order with which PNA probes were immobilized onto the metallic surface and samples with the same genotype were introduced into the microfluidic devices were changed from experiment to experiment.

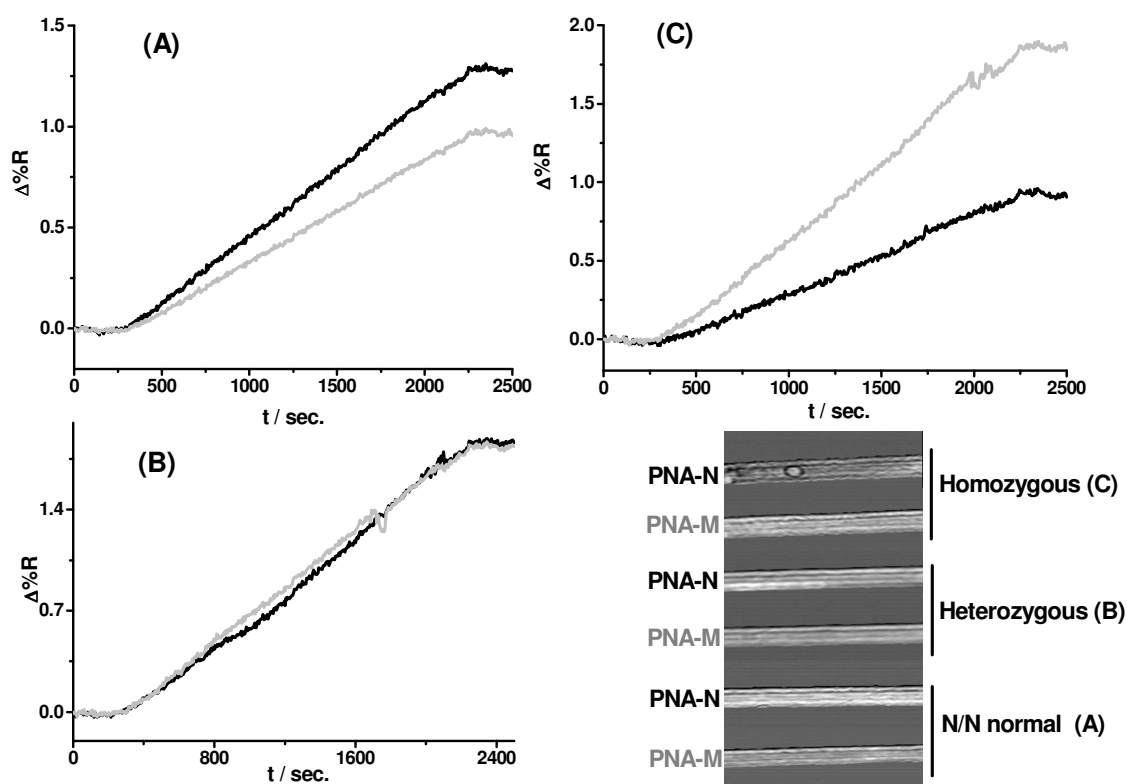


**Figure S5** Time-dependent SPRI curves obtained after the adsorption of conjugated AuNPs on normal  $\beta^N/\beta^N$  (A, sample 83), heterozygous  $\beta^{39}/\beta^N$  (B, sample 14) and homozygous  $\beta^{39}/\beta^{39}$  (C, sample 21) DNAs previously adsorbed to the surface immobilized PNA-N (black curve) and PNA-M (gray curve) probes.  $5 \text{ pg } \mu\text{L}^{-1}$  solutions of genomic DNAs were used for the experiments. A representative SPR difference image is also shown. In order to prevent memory effects the order with which PNA probes were immobilized onto the metallic surface and samples with the same genotype were introduced into the microfluidic devices were changed from experiment to experiment.

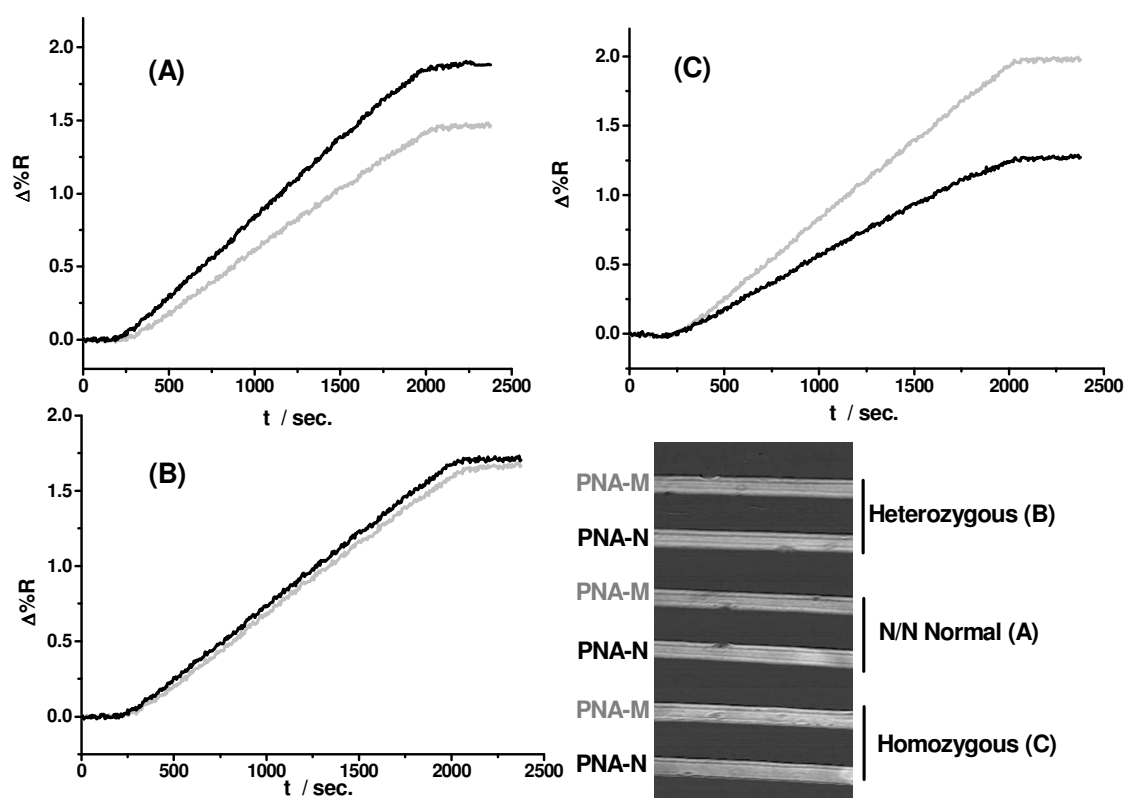


**Figure S6** Time-dependent SPRI curves obtained after the adsorption of conjugated AuNPs on normal  $\beta^N/\beta^N$  (A, sample 3P), heterozygous  $\beta^{o39}/\beta^N$  (B, sample 12) and homozygous  $\beta^{o39}/\beta^{o39}$  (C, sample 13) DNAs previously adsorbed to the surface immobilized PNA-N (black curve) and PNA-M (gray curve) probes.  $5 \text{ pg } \mu\text{L}^{-1}$  solutions of genomic DNAs were used for the experiments. A representative SPR difference image is also shown. In order to prevent memory effects the order with which PNA probes were immobilized onto the metallic surface and samples with the same genotype were introduced into the microfluidic devices were changed from experiment to experiment.



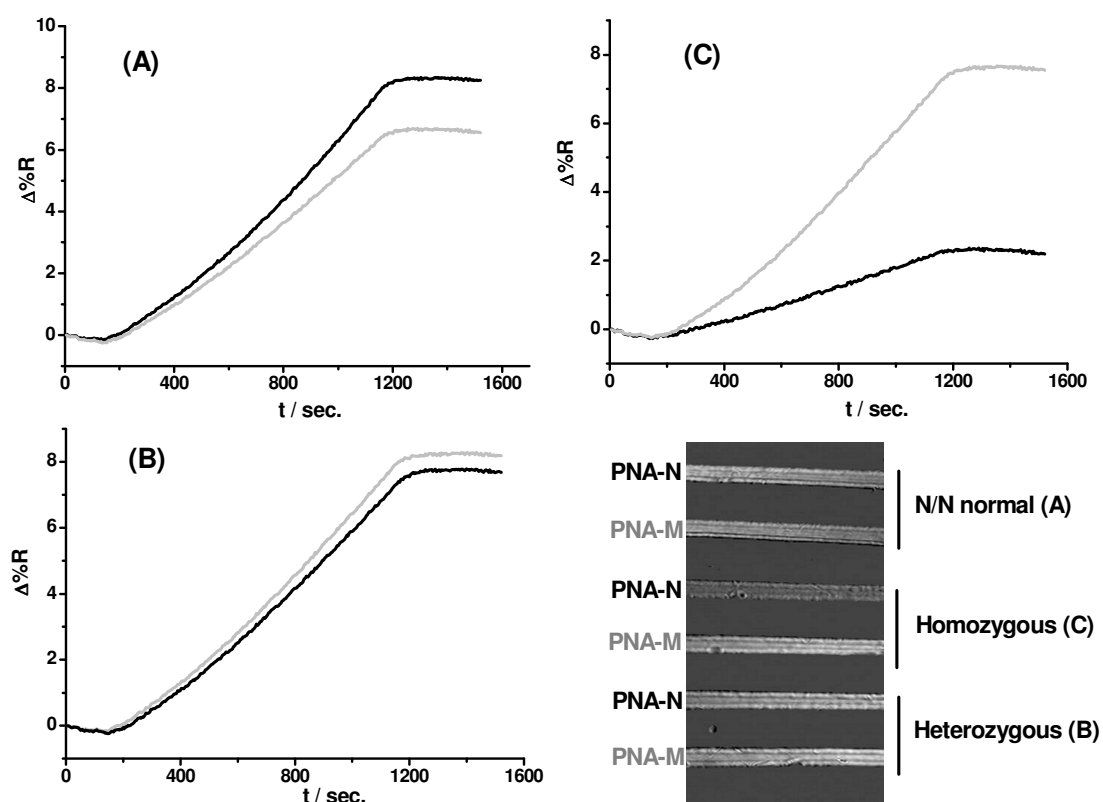


**Figure S7** Time-dependent SPRI curves obtained after the adsorption of conjugated AuNPs on normal  $\beta^N/\beta^N$  (A, sample 82), heterozygous  $\beta^{39}/\beta^N$  (B, sample 2) and homozygous  $\beta^{39}/\beta^{39}$  (C, sample 4) DNAs previously adsorbed to the surface immobilized PNA-N (black curve) and PNA-M (gray curve) probes.  $5 \text{ pg } \mu\text{L}^{-1}$  solutions of genomic DNAs were used for the experiments. A representative SPR difference is also shown. In order to prevent memory effects the order with which PNA probes were immobilized onto the metallic surface and samples with the same genotype were introduced into the microfluidic devices were changed from experiment to experiment.

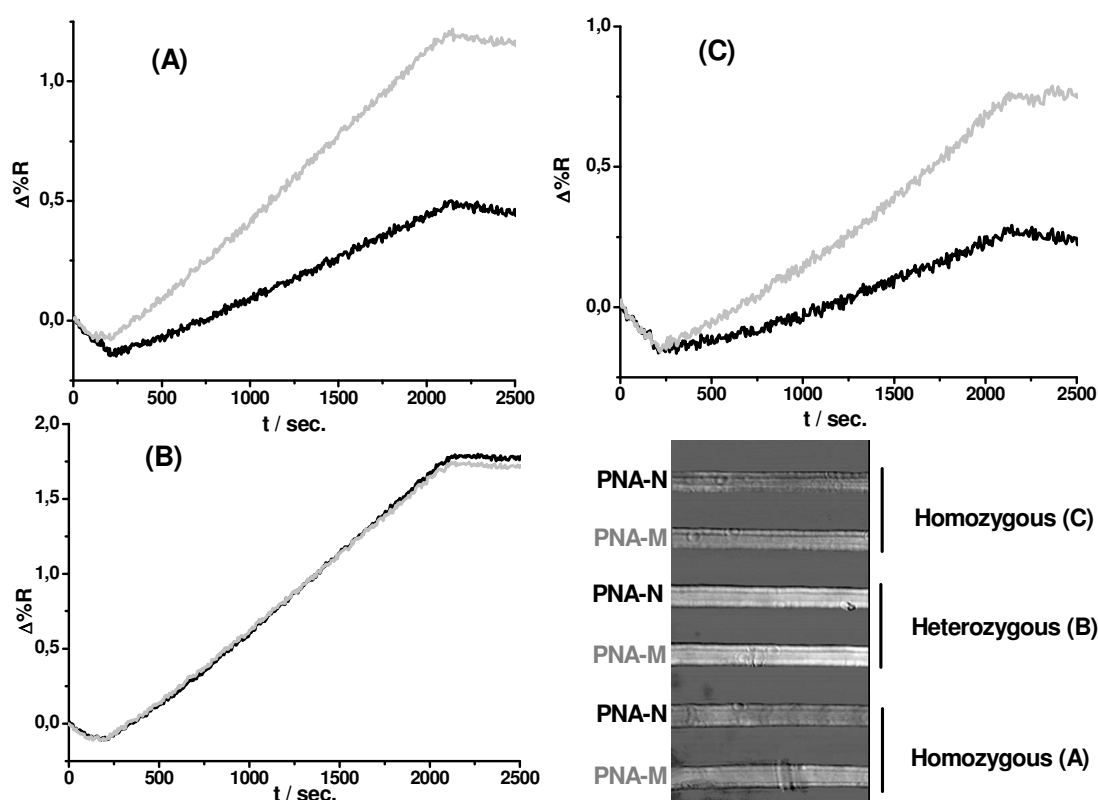


**Figure S8** Time-dependent SPRI curves obtained after the adsorption of conjugated AuNPs on homozygous  $\beta^{\circ}39/\beta^{\circ}39$  (A, sample 18), heterozygous  $\beta^{\circ}39/\beta N$  (B, sample 20) and homozygous  $\beta^{\circ}39/\beta^{\circ}39$  (C, sample 9) DNAs previously adsorbed to the surface immobilized PNA-N (black curve) and PNA-M (gray curve) probes.  $5 \text{ pg } \mu\text{L}^{-1}$  solutions of genomic DNAs were used for the experiments. A representative SPR difference image is also shown. In order to prevent memory effects the order with which PNA probes were immobilized onto the metallic surface and samples with the same genotype were introduced into the microfluidic devices were changed from experiment to experiment.

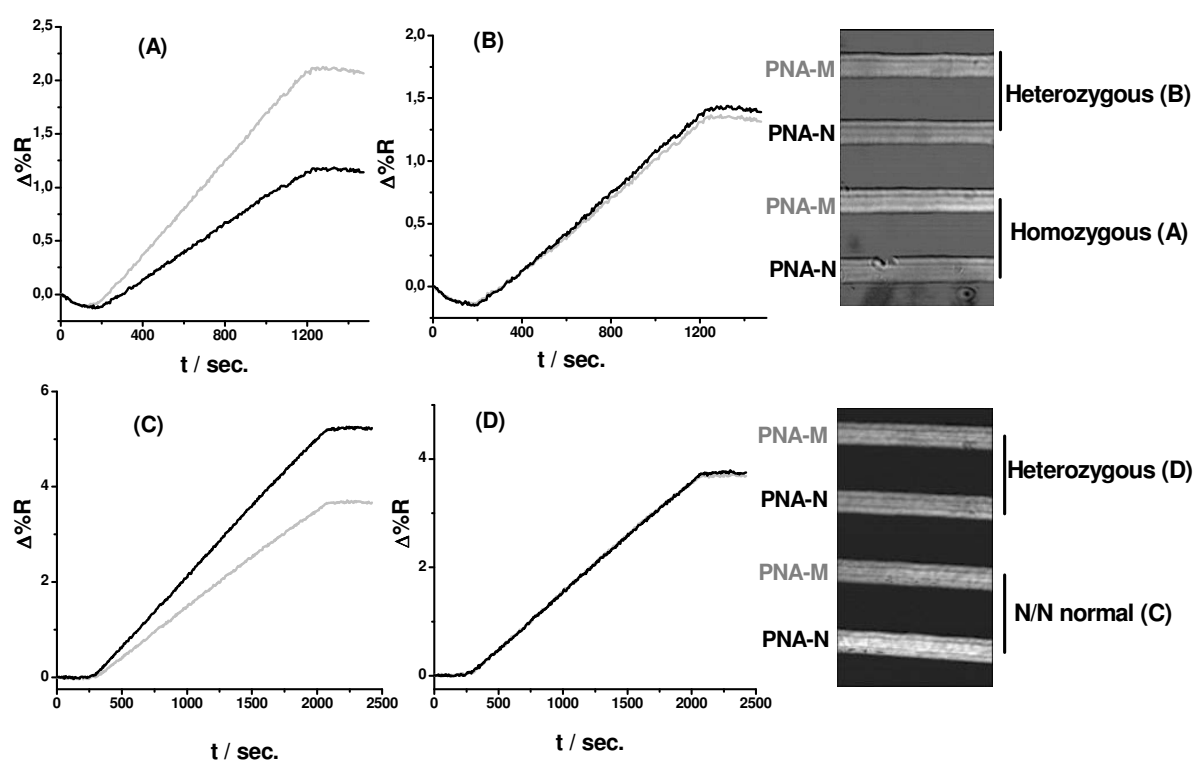


**Figure S9** Time-dependent SPRI curves obtained after the adsorption of conjugated AuNPs on homozygous  $\beta^{\circ}39/\beta^{\circ}39$  (A, sample 8), heterozygous  $\beta^{\circ}39/\beta^N$  (B, sample 7), normal  $\beta^N/\beta^N$  (C, sample 1), and heterozygous  $\beta^{\circ}39/\beta^N$  (D, sample 21) DNAs previously adsorbed to the surface immobilized PNA-N (black curve) and PNA-M (gray curve) probes.  $5 \text{ pg } \mu\text{L}^{-1}$  solutions of genomic DNAs were used for the experiments. Two representative SPR difference images are also shown. The SPR images show only four channels instead of six because the formation of air bubbles in some of the missing microchannels altered the integrity of the chip surface. In order to prevent memory effects the order with which PNA probes were immobilized onto the metallic surface and samples with the same genotype were introduced into the microfluidic devices were changed from experiment to experiment.

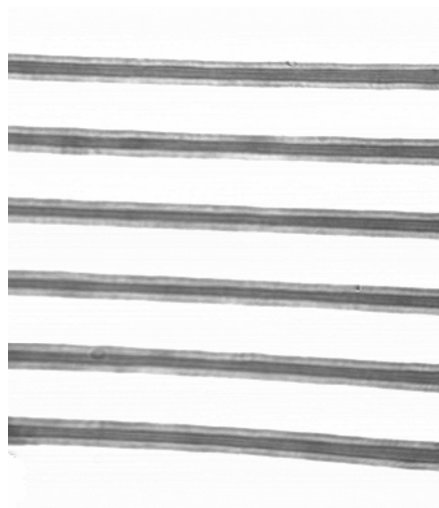


**Figure S10.** Representative SPRI image. The contrast was generated by the PBS running buffer continuous flow through six parallel microchannels.

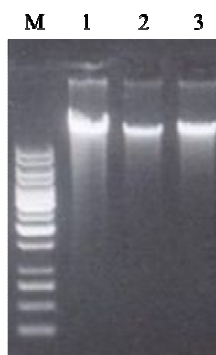


**Figure S11.** Representative 0.8% agarose gel electrophoretic analysis of genomic DNA samples (lanes 1, 2, 3). M, molecular weight ladder, 1kb DNA Ladder (10000, 8000, 6000, 5000, 4000, 3500, 3000, 2500, 2000, 1500, 1000, 750, 500, 250 bp) (Fermentas).

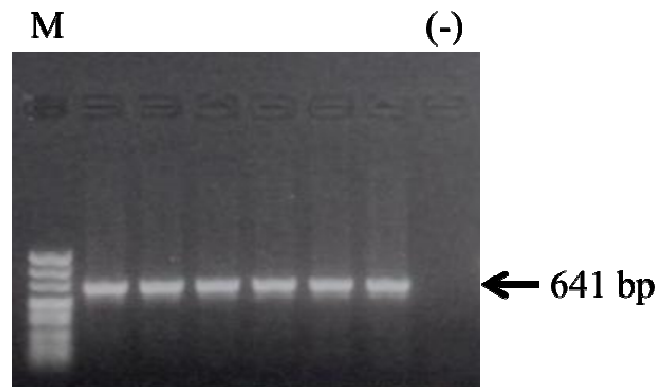


**Figure S12.** Agarose gel electrophoretic analysis of PCR products obtained by amplifying genomic DNA samples with primers BetaGlobinF and BetaGlobinR. The arrow indicates the position of the 641 bp specific amplification product. M, molecular weight ladder, pUC Mix Marker, 8 (1116, 883, 692, 501, 489, 404, 331, 242, 190, 147, 111, 110, 67 bp) (Fermentas). (-), negative control (water added to the amplification mixture).

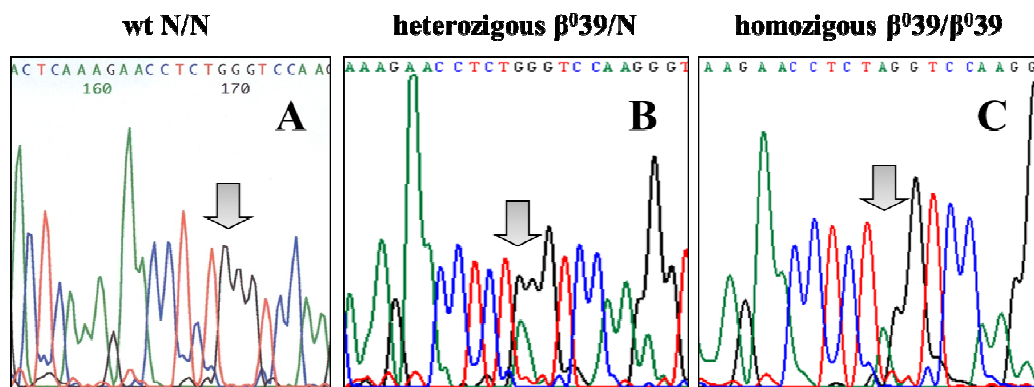


**Figure S13.** Representative portions of electropherograms obtained by sequencing BetaGlobinF-BetaGlobinR PCR products, obtained by wt N/N (A), heterozygous  $\beta^039/N$  (B), and homozygous  $\beta^039/\beta^039$  (C) DNA samples, with a reverse sequencing primer. Arrows indicate the peaks corresponding to the  $\beta^039$  position.